Aalborg Universitet

A Remedial Action Scheme to Prevent Mid/Long-Term Voltage Instabilities

Khoshkhoo, Hamid; Yari, Siavash; Pouryekta, Aref; Ramachandaramurthy, Vigna K.; Guerrero, Josep M.

A Remedial Action Scheme to Prevent Mid/Long-Term Voltage Instabilities

Hamid Khoshkhoo , Siavash Yari , Aref Pouryekta , *Member, IEEE,*
Vigna K. Ramachandaramurthy , *Senior Member, IEEE,* and Josep M. Guerrero , *Fellow, IEEE*

Abstract—The main objective of this article is to propose a special protection system (SPS) to execute efficient remedial actions to prevent mid-term and long-term voltage instabilities. In this method, when the operating point (OP) leaves the normal operation state, the proposed SPS is initiated to execute the required corrective remedial actions to bring the OP back to a normal state and maintain bus voltages above prespecified thresholds. Considering the local nature of Volt/Var control and in order to execute fast remedial actions, in this approach, the required generation rescheduling or load shedding procedures were selected based on the electrical distance concept. This allows for remedial actions with the highest impact on volt/var control. In addition, in generation rescheduling procedures, the proposed method uses the ability of utility-scale photovoltaic resources, which can change their generation quickly. This plays a major role in maintaining stability of power systems. Efficiency of the proposed algorithm was validated through several scenarios performed in IEEE 39-bus, Nordic32, and PST 16 test systems using DIgSILENT PowerFactory software. Results of these dynamic simulations and their comparison with some previously published methods show the effectiveness of this method in timely executing appropriate remedial actions to maintain system stability.

Index Terms—Large-scale photovoltaic (PV) power plants, power system stability, remedial action scheme, voltage stability.

I. INTRODUCTION

DURING the last decade, the considerable increase in system loading has pushed the power systems operating points (OPs) toward stability boundaries, indicating that voltage instability, also called load instability, has become a major threat to power systems [1]–[4]. Voltage instability occurs due to the inability of the power system to deliver the required power to load areas. This event is initiated when the limiters of synchronous generators (SGs) and other resources limit power generation or when the transmission system cannot transfer more power from generation areas to loads. In high loading conditions, on-load tap changers (OLTCs) that are used to regulate bus voltages may adversely affect the voltage of the target bus and result in more voltage drop leading to voltage instability [5], [6]. Therefore, to effectively analyze voltage stability, the capability of generation and transmission systems in generating and transferring more power to load areas, and the dynamic behavior of loads should be assessed.

In recent years, researchers have proposed control strategies such as special protection-based strategies to prevent instability. Based on the definition of the North American Electric Reliability Corporation, special protection system (SPS) (or remedial action scheme) indicates "*an automatic protection system designed to detect abnormal or predetermined system conditions, and takes corrective actions other than and/or in addition to the isolation of faulted components to maintain system reliability*" [7]. Among the different control strategies proposed in literature [8], SPS-based schemes seem to be more efficient in exploiting generation resources, system equipment (such as OLTCs, AVRs, and FACTS devices), load shedding, etc., to improve the stability stiffness of power networks that are large, complicated, and nonlinear [8]–[13]. Remedial actions executed in an SPS may be event-based, executed following particular contingencies, or response-based, which are performed when electrical variables or stability status indictors leave the normal operation state [14]. Although event-based schemes provide the chance for preventive actions (to bring the OP back to the region of attraction) against specified disturbances, response-based schemes are able to monitor the system state and perform remedial actions against any small and/or large disturbances.

Multiobjective optimization frameworks have been used to determine event-based remedial action schemes to prevent voltage instabilities [14]–[17]. With these methods, optimization algorithms have been used to determine the optimal amount and location of load shedding to improve voltage stability margins. In addition to load shedding, shunt capacitors, inductors, and SGs have been used in the proposed SPS to reduce the cost of load shedding [18]. Furthermore, a load shedding- based remedial action has been proposed in which the optimization problem is solved stage-by-stage to minimize the load-shedding amount as much as possible [19]. However, due to the dynamic behavior of power systems and the importance of executing timely remedial actions, it may be time-consuming and inefficient.

This article has been accepted for inclusion in a future issue of this journal. Content is final as presented, with the exception of pagination.

2

IEEE SYSTEMS JOURNAL

TABLE I
CHARACTERISTICS OF SPSs PROPOSED IN THE LITERATURE TO IMPROVE VOLTAGE STABILITY STATUS

Ref.	Voltage stability			Detection method		Implementation		Remedial actions					Assessment method based on		
	Short term	Mid term	Long term	Response based	Event based	Decentralized	Centralized	Load shedding	Generation rescheduling	FACTs control	OLTC control	LSPVPP/ VLSPVPP control	Generation system	Transmission system (line index)	Max. loadability (Voltage of buses, bus index....)
[6]	×	✓	✓	✓	×	✓	×	✓	×	×	×	×	✓	×	✓
[14]	×	×	✓	×	✓	×	✓	✓	×	×	×	×	×	×	×
[15]	×	×	✓	×	✓	×	✓	✓	×	×	×	×	×	×	×
[16]	×	×	✓	×	✓	×	✓	✓	×	×	×	×	×	×	×
[17]	×	×	✓	×	✓	×	✓	✓	×	×	×	×	×	×	×
[18]	×	×	✓	×	✓	×	✓	✓	×	✓	×	×	×	×	×
[19]	×	×	✓	×	✓	×	✓	✓	×	×	×	×	×	×	×
[20]	×	×	✓	✓	✓	×	✓	✓	✓	×	×	×	×	×	✓
[21]	×	×	✓	✓	×	✓	×	✓	×	×	×	×	✓	×	✓
[22]	×	×	✓	✓	×	✓	×	✓	×	×	×	×	×	✓	✓
[23]	×	✓	✓	✓	×	✓	×	✓	×	×	×	×	✓	×	✓
The proposed Method	×	✓	✓	✓	×	✓	×	✓	✓	×	✓	✓	✓	✓	✓

In [6], the power system has been divided into several voltage control areas (VCAs) and a stability index, namely *PI*, was used to assess the stability status of each VCA. A response-based load shedding scheme was then executed to prevent the *PI* index from reaching its critical threshold. Nevertheless, in selecting the required remedial actions, this method did not consider the capability of transmission systems to transfer power to load areas. Neglecting the capability of generation and distribution systems, the integral square voltage magnitude indicator, based on bus voltages measured by phasor measurement unit (PMUs), has been suggested to perform response-based remedial actions [20]. An adaptive load shedding method has also been presented [21], in which the load shedding amount is determined according to the system frequency and the voltage falling rate to preserve the frequency and voltage stability of the power system. However, the main drawback of this method is that the amount and location of load shedding are nonoptimal. A response-based SPS, which uses decentralized load shedding schemes to prevent voltage instability, has been proposed [22], [23]. Nevertheless, these methods (expect [22]) do not consider the capability of the transmission system in delivering the required power to loads.

Table I gives the SPS-based methods proposed in the literature to improve voltage stability along with their technical criteria and those tools used in each method. Although they have used different schemes to improve performance of remedial actions and reduce the cost of maintaining system stability, they have not considered all aspects of the voltage inability. In addition, the methods did not utilize all available tools in the prevention of voltage instability. For instance, these methods did not consider OLTCs, which may jeopardize voltage stability status.

In this respect, it seems that proposing an SPS which considers the impacts of generation and transmission systems on the voltage instability phenomenon and utilizes all available tools to execute coordinated remedial actions is an important step towards implementing cost-effective measures to prevent system instability. Obviously, such a remedial action scheme should have low computation burden (for example, without optimization algorithms which are time-consuming) to timely track the post disturbance stability status and perform the required corrective control actions. In addition, such an SPS should utilize all available remedial action in a coordinated manner to minimize the amount of load-shedding.

In 2017, the capacity of large-scale photovoltaic (PV) power plants (LSPVPP with a minimum size of 1 MW) and very large-scale PV power plants (VLSPVPP with a minimum size of 100 MW) reached almost 239 GW and it is expected that their capacity will increase by 320 GW (about 32% of the total growth of renewable capacity) before 2024 [24]–[26]. Since these resources are installed in transmission systems and can affect the stability status of networks, in future power systems where the capacity of them will increase significantly, they should support the grid in terms of frequency, voltage, active, and reactive power regulation to enhance the system stability. Accordingly, it seems that analyzing the impacts of these resources on system stability and utilizing their capabilities in improving system stability is inevitable.

Based on extensive investigation by the authors, the assessment of the impacts of these resources on system stability status is limited to a few works [27]–[30], and their capabilities have not, as yet, been utilized by any proper SPS to prevent voltage instability. From an electrical point of view, the main feature of PV resources is their ability to quickly increase or decrease their active and reactive power generation [27]. Hence, they seem to be a proper tool to execute fast corrective actions that are vital in maintaining the OP in the region of attraction.

Based on the above-mentioned research gap, this article aims to propose a SPS which considers the impacts of both generation and transmission systems on the voltage stability status and (considering the disturbance severity) utilizes required remedial actions as well as the capabilities of LSPVPP to execute timely and coordinated optimal corrective actions to minimize the load-shedding amount. Therefore, the main contribution of this paper is to propose a SPS that:

1) has low computational burden to continuously assess the post-disturbance stability status and select the required remedial actions. Thus, it can be suitable for online applications;

2) considers the impacts of generation system, transmission system, and system loading condition on the voltage stability to accurately assess the postdisturbance stability stiffness;

3) utilizes the capabilities of LSPVPP to take fast corrective remedial measures to enhance dynamic stability status;

4) based on the disturbance severity, utilizes all available remedial actions in a coordinated manner to either bring back the OP to the region of attraction without any load shedding or significantly decreases the required load shedding amount.

In this article, an SPS with low computational burden is proposed to overcome the aforementioned drawbacks, considering the local nature of voltage and reactive power control. The proposed method divides the network into several VCAs and continuously checks the stability status of each VCA. Then, for any small and/or large disturbances that cause the system variables to hit the predefined thresholds, starting from the nearest resources (conventional and PV resources) to the low voltage buses and/or critical transmission lines, the generation of resources is regulated to improve system stability. If this generation rescheduling cannot bring the OP back to the Normal state, load-shedding is executed to shed the minimum amount of those loads that adversely affect the stability status and maintain system stability.

The rest of this article is organized as follows. Section II provides the required tools for the proposed method. In this section, network partitioning into several VCAs, identification of weak buses using bus stability index simplified voltage stability index (SVSI), assessment of the stability status using the improved line stability index (ILSZ), and analysis of the capability of an SG to generate more reactive power using reactive power reserve index (RPRI) will be explained briefly. Also, modeling of the utility-scale PV resources in DIgSILENT PowerFactory software is explained. In Section III, the proposed SPS is explained, and Section IV will provide the simulation results. Finally, conclusions are presented in Section V.

II. REQUIRED TOOLS

A. Power System Partitioning and VCA Concept

For voltage stability assessment, it seems logical to partition the system into several VCAs and estimate the closeness of resources and loads to regions affected by the disturbance to estimate their impacts on voltage stability [31]. In this article, the electrical distance (ED) concept has been used to determine VCAs in power systems. In this method, the ED between bus n and bus m is calculated as follows, and each VCA includes those buses that are close to each other:

$$\text{ED}_{mn} = \text{ED}_{nm} = -\log(a_{mn} \times a_{nm}) \tag{1}$$

where a_{mn} and a_{nm} can be calculated using the load flow Jacobian matrix [32] or the susceptance matrix [33]

$$a_{mn} = \left(\frac{\partial V_m}{\partial Q_n}\right) \bigg/ \left(\frac{\partial V_n}{\partial Q_n}\right) \, a_{nm} = \left(\frac{\partial V_n}{\partial Q_m}\right) \bigg/ \left(\frac{\partial V_m}{\partial Q_m}\right). \tag{2}$$

TABLE II
THRESHOLD VALUES FOR ILSZ INDEX TO CLASSIFY THE STABILITY STATUS [35]

Index	Thresholds		
	Normal (Margin>30%)	Alert (20%<Margin<30%)	Emergency (Margin<20%)
ILSZ	*ILSZ*< 0.54	0.54 <*ILSZ*< 0.67	*ILSZ*> 0.67

B. Determination of VLSPVPP Locations Using SVSI

In this article, to assess the performance of the proposed SPS in different test systems, it is assumed that VLSPVPP was installed at weak buses that can be determined using SVSI [34]. In this regard, system loading increases consecutively, and at the maximum loading point, SVSI is calculated for all buses to determine those buses (in each VCA) whose SVSI are more than other ones [34]

$$\text{SVSI}_i = \frac{\Delta V_i}{\beta \times V_i} = \frac{\left|\vec{V}_g - \vec{V}_i\right|}{\beta \times V_i} \tag{3}$$

where V_i is the voltage of bus i, V_g is the terminal voltage of the nearest generator to bus i (determined using the ED), and β, is the correction factor [34].

C. Assessment of Voltage Stability Status Using ILSZ

The main drawback of line stability indices is that they can only assess stability in simple two-bus systems and they are not able to properly assess the stability status in real networks [35]. Thus, the authors have proposed an improved line stability index in [35], i.e., ILSZ, and improved its calculation procedure to accurately assess the stability status in real networks [22]. The ILSZ for line i is calculated by

$$\text{ILSZ}_i = \frac{2\left|Z_i + Z_{\text{th}}\right|\left|S_r\right|}{\left|E_{\text{th}}\right|^2 - 2\left|Z_i + Z_{\text{th}}\right|(p_r \cos\theta_{\text{th}} + Q_r \sin\theta_{\text{th}})} \tag{4}$$

where Z_i is the impedance of the Line i, E_{th} is the terminal voltage of the nearest generator to the sending bus of Line i, and Z_{th} is the total impedance of the shortest path from the sending bus of line i to the nearest generator. It should be stated that, based on voltage magnitude criteria, among those buses across line i, the one whose voltage magnitude is greater than the other bus is selected as the sending bus [35], [36]. Critical value of ILSZ is unity, which means that, as the power passing through the line reaches the maximum transferrable power, ILSZ gets closer to unity. Obviously, those lines whose ILSZ is close to unity are the more critical ones. It should be stated that ILSZ uses those thresholds mentioned in Table II, to classify the stability status into *normal*, *alert*, and *emergency*, which indicate the loadability margin of the critical transmission lines [35].

D. Assessment of SGs Using RPRI

Under high loading conditions, reactive generation of an SG increases to control the terminal voltage. However, when the reactive power reaches its limit, the SG will operate in *PQ* mode and can no longer control the terminal voltage.
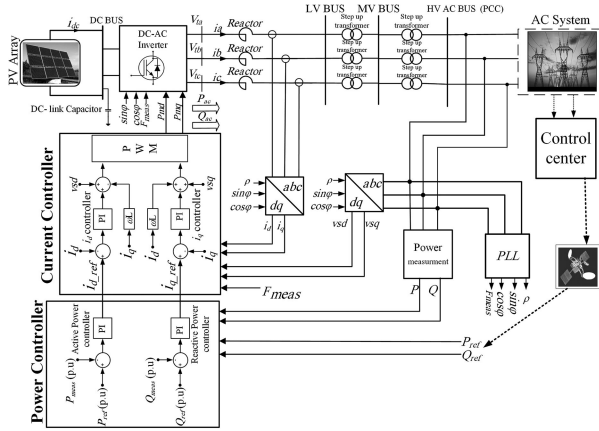
Fig. 1.   Decouple control method used to regulate the output active and reactive power of VLSPVPP.

Fig. 2.   Flowchart of the proposed SPS to prevent mid/long-term voltage instabilities.

Therefore, calculating the reactive power generated by SGs at any moment and comparing it with its maximum value is inevitable to analyze stability status and to choose optimal remedial actions. For this purpose, RPRI index has been proposed as follows to quantify the amount of extra reactive power that a generator can produce [37]

$$\text{RPRI} = \min i \in G \left(\frac{Q_i^{\max} - Q_i}{Q_i^{\max}} \right) \tag{5}$$

where Q_i is the reactive power generated by the SG, and $Q_i^{\max}$ is the maximum reactive power which can be generated by SG [6]. Clearly, those SGs whose RPRI reach zero can no longer generate reactive power and contribute to voltage stability control.

E. Modeling of VLSPVPP

With the advancement in power electronics and semiconductor technology, voltage source converters are now more popular to integrate PV resources and energy storage systems into high voltage systems. According to the European Solar Association, PV penetration will reach 32% in 2030 across the European countries [27]. Generally, small inverters are connected into the distribution systems while VLSPVPPs are connected into the transmission systems via step up transformers. Although distributed generators connected into the distribution network are not allowed to regulate the voltage at point of common coupling (PCC), VLSPVPP plants, which are connected to the high voltage network, are permitted to operate in *P–V* control mode [38]. Clearly, these resources can increase their reactive power up to their rating value. In this article, the decoupled-*dq* control method (illustrated in Fig. 1 and implemented in the dynamic simulation language environment of *PowerFactory* software) is used to control the voltage and output power of VLSPVPP [39].

III. PROPOSED PROTECTION SYSTEM

In this section, to prevent voltage instability, an effective response-based SPS algorithm with low computational burden is proposed. In this method, the network is divided into several VCAs and the ILSZ index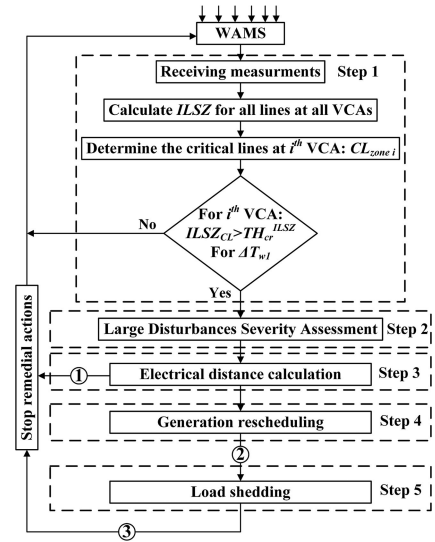 continuously assesses the stability status of the network and triggers the proposed SPS if the ILSZ value of any lines (i.e. critical lines, ILSZ$_{\text{CL}}$) reaches $\text{TH}_{cr}^{ILSZ}(=0.54)$ and stays above this threshold for ΔT_{w1} s. The flowchart of the proposed SPS, given in Fig. 2, indicates that it includes two main stages for generation rescheduling and load shedding which may be explained as follows.

Step1: Continuous Stability Assessment:

At each OP, receive the time-synchronized measured data provided by WAMS and determine the critical areas (VCA_i) where the ILSZ values of some lines (namely critical lines, $\text{CL}_{\text{zone}i}$) exceed the critical threshold TH_{cr}^{ILSZ} during the last ΔT_{w1} s. If there are any critical areas, go to the next step, otherwise repeat this step.

Step 2: Large Disturbances Severity Assessment:

If a large disturbance has occurred, calculate the amount of power shortage after ΔT_{w1} s in all critical areas as follows:

$$P_{sh}^i = \sum_{\text{TL}} P_{\text{TL,pre}}^i - \sum_{\text{TL}} P_{\text{TL,post}}^i \tag{6}$$

where $P_{\text{TL,pre}}^i$ and $P_{\text{TL,post}}^i$ is the amount of active power transferred to the *i*th VCA (through tie lines) before and ΔT_{w1} s after the contingency occurrence, and P_{sh}^i is the power shortage in *i*th VCA, respectively.

Step 3: ED Calculation:

In all critical areas, calculate the EDs between buses.

Step 4: Generation Rescheduling:

The flowchart of this step, which is executed in critical areas, is shown in Fig. 3. According to this figure we can understand the next steps as following.

Steps 4–1: If a large disturbance has occurred and the rate of change of frequency (ROCOF) becomes $>\text{TH}_{cr}^{ROCOF}$ (during ΔT_{ROCOF} s after the
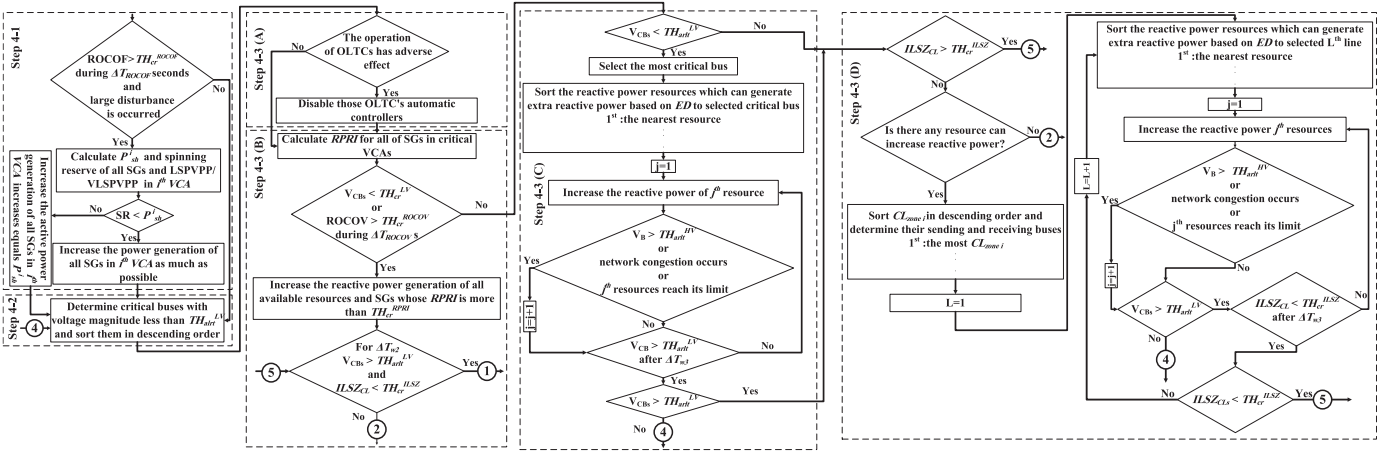
This article has been accepted for inclusion in a future issue of this journal. Content is final as presented, with the exception of pagination.

KHOSHKHOO et al.: REMEDIAL ACTION SCHEME TO PREVENT MID/LONG-TERM VOLTAGE INSTABILITIES 5

Fig. 3. Step 4 of the proposed SPS shown in Fig. 2.

ILSZ value of any critical lines, ILSZ_{CLs}, reaches TH_{cr}^{ILSZ}), determine the spinning reserve of all SGs and VLSPVPP in ith VCA. If this reserve is $> P_{\text{sh}}^i$, increase the active power of generation units in ith VCA so that the total generation increment equals P_{sh}^i. Otherwise, if the reserve in the ith VCA is $< P_{\text{sh}}^i$, increase the power generation of all generation units in the ith VCA as much as possible.

Steps 4–2: In each critical area, determine those buses whose voltage magnitudes are $<$ a threshold $\text{TH}_{\text{alrt}}^{\text{LV}}$ (i.e., critical buses) and sort them in descending order.

Steps 4–3: In any critical areas as follows:

Steps 4–3(A): If the operation of any OLTC jeopardizes stability status, disable those OLTC's automatic controllers until the end of step 4 (it should be stated that the algorithm continuously monitors OLTCs operation).

Steps 4–3(B): If the voltage of any critical bus (V_{CBs}) becomes $< \text{TH}_{cr}^{\text{LV}}$ or the rate of change of voltage (ROCOV) become more than a threshold $\text{TH}_{cr}^{\text{ROCOV}}$ during ΔT_{ROCOV} s after the moment that ILSZ_{CLs} reaches TH_{cr}^{ILSZ}, increase the reactive power generation of all resources (which can generate more reactive power) as much as possible. In this regard, all VLSPVPP, capacitor banks, and SGs whose RPRI values are $> \text{TH}_{cr}^{\text{RPRI}}$ should increase their reactive power. Then, if the voltage magnitude of all buses exceeds $\text{TH}_{\text{alrt}}^{\text{LV}}$ and ILSZ_{CLs} become $< \text{TH}_{cr}^{ILSZ}$ for ΔT_{w2} s, stop the remedial actions and enable the OLTC's controllers. Otherwise, go to step 5 (load shedding procedure).

Steps 4–3(C): Otherwise, if the V_{CBs} become $< \text{TH}_{\text{alrt}}^{\text{LV}}$ (and $> \text{TH}_{cr}^{\text{LV}}$), starting from the first critical bus (i.e., the most critical one obtained in steps 4–2), sort those resources that can generate more reactive power (VLSPVPP, capacitor bank, or SGs whose RPRI is $> \text{TH}_{\text{alrt}}^{\text{RPRI}}$) based on

their ED to the intended critical bus. Then, starting from the nearest resource, increase reactive power generation until the voltage of the intended critical bus (V_{CB}) become $> \text{TH}_{\text{alrt}}^{\text{LV}}$, or the voltage of any bus (V_{B}) becomes $>$ the thresholds $\text{TH}_{\text{alrt}}^{\text{HV}}$, or network congestion occurs. If, ΔT_{w3} s after increasing the reactive power of the selected resource, V_{CB} still remains $< \text{TH}_{\text{alrt}}^{\text{LV}}$ (and $> \text{TH}_{cr}^{\text{LV}}$), select the next reactive power resource. Otherwise, if V_{CBs} still remains $< \text{TH}_{\text{alrt}}^{\text{LV}}$, go back to steps 4-2.

Steps 4–3(D): If there are any critical lines (whose ILSZ value is $> \text{TH}_{cr}^{ILSZ}$), sort them in descending order and determine their sending and receiving buses by the voltage magnitude criterion [35], [36]. Starting from the first critical line (the most critical one), sort the reactive power resources that can generate more reactive power, based on their ED, to the receiving bus of the intended critical line. Then, starting from the nearest resource, increase their reactive power one by one. After ΔT_{w3} s, if ILSZ_{CL} becomes $< \text{TH}_{cr}^{ILSZ}$, select the next critical line and repeat the above-mentioned procedure. Otherwise, if the resource cannot generate extra reactive power, or the V_{B} becomes $> \text{TH}_{\text{alrt}}^{\text{HV}}$, or network congestion occurs, select the next reactive power resource and go back to steps 4–2.

If, during the ΔT_{w2}s, ILSZ_{CLs} in all critical areas become $< \text{TH}_{cr}^{ILSZ}$ and the voltage magnitudes of all buses become $> \text{TH}_{\text{alrt}}^{\text{LV}}$, stop the remedial actions and enable OLTC's.

Step 5: Load Shedding:

The flowchart of this step, which is executed in critical areas, is shown in Fig. 4, and may be described as follows. It should be stated that, in this step, along with executing the following procedures, the proposed algorithm checks the operation of OLTCs. If the operation of any OLTCs jeopardizes stability
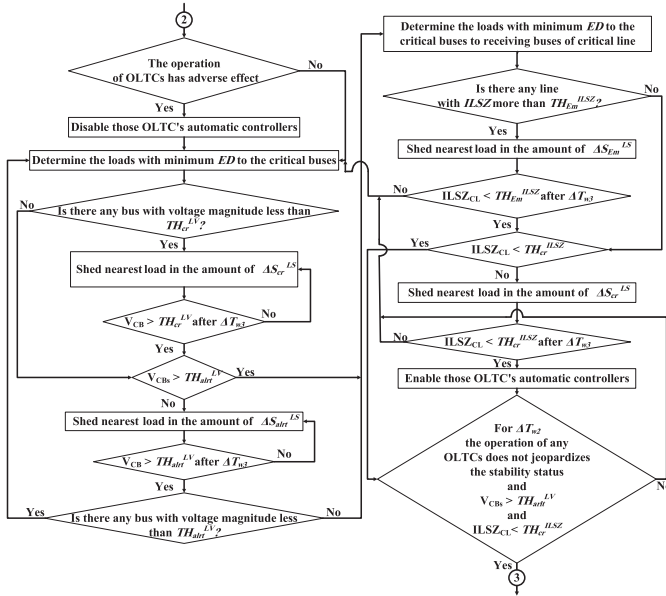
This article has been accepted for inclusion in a future issue of this journal. Content is final as presented, with the exception of pagination.

6   IEEE SYSTEMS JOURNAL

Fig. 4.   Step 5 of the proposed SPS shown in Fig. 2.

Threshold	TH_{cr}^{ILSZ}	TH_{Em}^{ILSZ}	TH_{alrt}^{LV}	TH_{cr}^{LV}	TH_{cr}^{ROCOV}	TH_{cr}^{ROCOF}
Value	0.54	0.67	0.96pu	0.93pu	1%	1%
Threshold	TH_{cr}^{RPRI}	TH_{alrt}^{HV}	ΔS_{alrt}^{LS}	ΔS_{cr}^{LS}	ΔS_{em}^{LS}	-
Value	5%	1.05pu	1%	3%	5%	-
Threshold	ΔT_{ROCOV}	ΔT_{ROCOF}	ΔT_{w1}	ΔT_{w2}	ΔT_{w3}	-
Value	10s	10s	10s	20s	5s	-

generation and transmission (i.e., lines and OLTCs) systems on the stability stiffness. Therefore, unlike some previously published SPSs which include time-consuming calculations (e.g., optimization algorithms), the proposed procedure is suitable for online application.

Also, as described in step 4, based on the disturbance severity, firstly coordinated remedial actions (except load shedding) are executed to maintain the system stability. In this respect, against most of the previously published research works, the proposed method, primarily perform coordinated remedial actions to enhance the stability status without any load shedding. Furthermore, since the capacity of LSPVPP will significantly increase in next decades, in the proposed SPS, these resources will operate similar to conventional power plants and contribute to enhance system stability.

However, if generation and transmission systems cannot meet post-disturbance loading condition, based on the local nature of volt/var control, ED concept is used to perform the least possible amount of load shedding.

It should be stated that in this article the time interval ΔT_{w3} $(= 5)$ s is selected so that it is long enough to check the stability status, but short enough to perform timely remedial actions and avoid delayed remedial actions. Also, to stop remedial actions, during the next ΔT_{w2} s after performing remedial actions, the algorithm check the stability status to assure that generation systems, transmission systems, OLTCs (with slow dynamic response) and load behavior do not again jeopardize the system stability. Therefore, in this paper it is assumed that $\Delta T_{w2} = 20$ s which is more than twice the operation time of OLTC (=8 s).

In addition, it is noteworthy that the proposed SPS is response-based (not event-based) and it continuously assess the stability status. Therefore, if any unexpected factors threaten the system stability, this SPS again begins to perform the remedial actions to improve the system stability.

status, disable these OLTC's automatic controllers temporarily. In any critical areas:

1) If V_{CBs} become $< TH_{cr}^{LV}$, determine loads with minimum ED to the critical buses and shed ΔS_{cr}^{LS} of these loads. It is worth mentioning that if a load is the nearest one to more than one critical bus, only shed ΔS_{cr}^{LS} of that load. Check the voltage magnitude the of above-mentioned buses during the next ΔT_{w3} s and repeat this procedure if the voltage of any critical bus is still $< TH_{cr}^{LV}$.

2) If the voltage magnitude of any critical buses becomes $> TH_{cr}^{LV}$ and still $< TH_{alrt}^{LV}$, determine loads with minimum ED to the critical buses and shed ΔS_{alrt}^{LS} of these loads. Again, check the voltage magnitude of above-mentioned buses during the next ΔT_{w3} s and repeat the procedure if V_{CBs} are still $< TH_{alrt}^{LV}$. If the voltage magnitude of any buses becomes $< TH_{alrt}^{LV}$, go back to the beginning of step 5.

3) If $ILSZ_{CLs}$ is $> TH_{cr}^{ILSZ}$ (TH_{Em}^{ILSZ}), determine their sending and receiving buses by the voltage magnitude criterion [35], and determine loads with minimum ED to their receiving buses and shed ΔS_{cr}^{LS} (ΔS_{em}^{LS}) of these loads. It is worth mentioning that if a load is the nearest load to more than one line, only shed ΔS_{cr}^{LS} (ΔS_{em}^{LS}) of that load. Again, check $ILSZ_{CLs}$ during the next ΔT_{w3} s and go to the beginning of step 5 if the ILSZ values of any critical lines remain $> TH_{cr}^{ILSZ}$.

4) Enable the OLTCs' automatic controllers. Then, during the next ΔT_{w2} s, if OLTCs do not jeopardize stability status, the voltage magnitude of all buses become $> TH_{alrt}^{LV}$, and $ILSZ_{CLs}$ becomes $< TH_{cr}^{ILSZ}$, stop the remedial actions. Otherwise, go to the beginning of step 5.

According to this algorithm, the proposed SPS uses simple decision-making criteria with low computational to continuously assess the stability status and analyze the impact of the

IV. SIMULATION RESULTS

For this section, the proposed SPS was implemented and tested on IEEE 39-bus, Nordic32, and PST 16 test systems to check the performance of the proposed remedial action scheme in preventing mid- and long-term voltage instability. In this respect, these test systems were implemented in DIgSILENT PowerFactory software. Controllers of SGs (AVRs, governors, and PSSs) and OLTCs, PV power plants, and voltage-dependent loads were modeled to accurately simulate dynamic behavior of the power networks. According to following remarks, values of thresholds used in these simulations are given in Table III.

1) As mentioned in [35], $\text{TH}_{cr}^{ILSZ} = 0.54$, $\text{TH}_{Em}^{ILSZ} = 0.67$ indicates the stability margins: "20<margin<30%" and "margin <20%", respectively, which are used in this article to determine the stability stiffness.

2) In high voltage systems (e.g. 400 kV), voltage variation of $\pm 10\%$ (under abnormal condition) and $\pm 5\%$ (under normal condition) are usually permissible. Accordingly, in this article, it is assumed that $\text{TH}_{cr}^{LV} = 0.93$, $\text{TH}_{alrt}^{LV} = 0.96$, and $\text{TH}_{alrt}^{HV} = 1.05$ to assure that the system operation is acceptable. Also, it should be stated that $\text{TH}_{alrt}^{LV} = 0.96$ equals to minimum acceptable voltage of those buses controlled by OLTC transformers to assure that the continuous operating voltage is within acceptable limits.

3) TH_{cr}^{ROCOF} and TH_{cr}^{ROCOV} are system specific and as these parameters increase, more load-shedding will be executed. In this manuscript, according to extensive simulation results and thresholds mentioned in the literature, it is assumed that $\text{TH}_{cr}^{ROCOV} = 1\%$, $\text{TH}_{cr}^{ROCOF} = 1\%$.

4) Considering the margin of 5%, $\text{TH}_{cr}^{RPRI} = 0.05$ is used to detect those generators which generate their maximum reactive power.

5) In this article, load shedding amount (which is system specific) is selected based on the stability status (i.e. alert, critical, and emergency) to take appropriate corrective actions. Accordingly, in the following simulations, it is assumed that $\Delta S_{alrt}^{LS} = 1\%$, $\Delta S_{cr}^{LS} = 3\%$, $\Delta S_{em}^{LS} = 5\%$.

6) In the proposed approach, ΔT_{w1}, ΔT_{w2}, and ΔT_{w3} (which are system specific) determine the time interval for checking the stability status in different steps of the proposed algorithm. Therefore, in this article, $\Delta T_{w1} = 10$ s is large enough to assure that the occurred disturbance has jeopardized the system stability and also, prevent any unnecessary remedial actions. Also, $\Delta T_{w2} = 20$ s is more than twice the operation time of OLTC (=8 s) to assure that OLTC transformers (with slow dynamic response) do not have any adverse impact on the stability status. Finally, $\Delta T_{w3} = 5$ s is long enough to check the stability status, but short enough to perform timely remedial actions and avoid delayed remedial actions.

Among different dynamic simulations perform by authors, in following subsections the performance of the proposed SPS in three scenarios will be proposed.

A. Analyzing Performance of the Proposed SPS Against Outage of Line 21–22 in IEEE 39-Bus Test System (Scenario 1)

In this section, a modified version of the IEEE 39-bus test system was used to analyze the performance of the proposed scheme. As mentioned in Section II, based on the method described in [33], this network was divided into three VCAs and in each VCA, the criterion "SVSI>0.8" was used to determine weak buses where VLSPVPP was installed. As given in Table IV, since there was no weak bus in VCA 1, utility-scale PV resources were installed in VCA 2 and VCA 3 (with a penetration level of 25%), which is given in Table IV and shown in Fig. 5. Also in this modified test system, each load was connected to the

TABLE IV
CRITICAL BUSES AND THE UTILITY-SCALE PV RESOURCES INSTALLED IN EACH VCA.

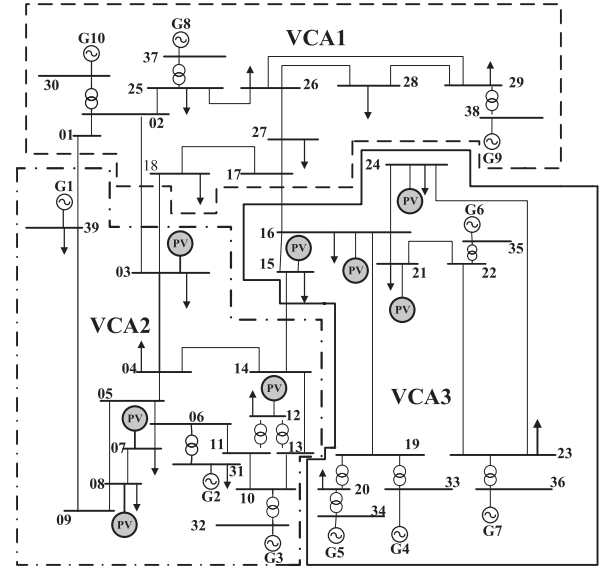| VCA		Critical buses			
VCA 1	Bus#	Bus27	Bus18	Bus28	Bus26
	SVSI	0.71	0.67	0.5	0.42
	Installed PV	-	-	-	-
VCA 2	Bus	Bus12	Bus08	Bus07	Bus03
	SVSI	0.97	0.89	0.85	0.84
	Installed PV	135.75$^{\text{MVA}}$	135.75$^{\text{MVA}}$	135.75$^{\text{MVA}}$	135.75$^{\text{MVA}}$
VCA 3	Bus	Bus15	Bus16	Bus21	Bus24
	SVSI	0.94	0.90	0.89	0.81
	Installed PV	131.25$^{\text{MVA}}$	131.25$^{\text{MVA}}$	131.25$^{\text{MVA}}$	131.25$^{\text{MVA}}$

Fig. 5. IEEE 39-bus test system is divided into three VCAs and utility-scale PV resources installed in VCA 2 and VCA 3.
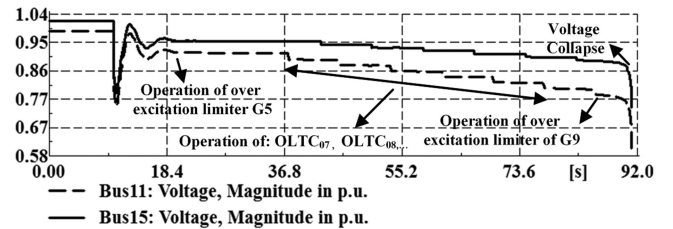

Fig. 6. Bus voltages in scenario 1 without proposed SPS.

transmission system through an OLTC, and those transformers connected between buses 11 and 12, buses 13–15, and buses 20–19 had an OLTC.

As shown in Fig. 6, in this scenario, the line 21–22 outage has occurred at $t = 10$ s and caused the overexcitation limiter of generator G5 to activate, which limited the reactive power generation of this SG. Also, voltage drop caused some OLTCs to automatically change their tap positions to improve voltage profile. However, these changes resulted in more voltage drop and lead to activation of over-excitation limiters of SGs G9, G1, G3. Eventually, the voltage collapse occurred at $t = 90$ s.

Fig. 7 shows that applying the proposed algorithm can properly prevent the OP to leave the region of attraction and cause the network to reach a stable equilibrium point. As shown in
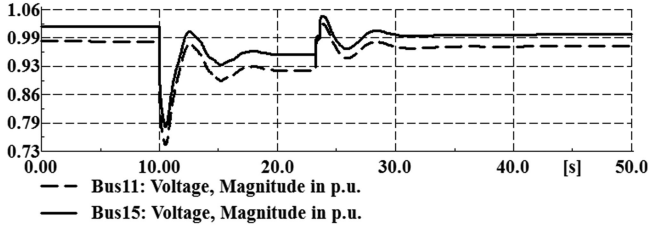
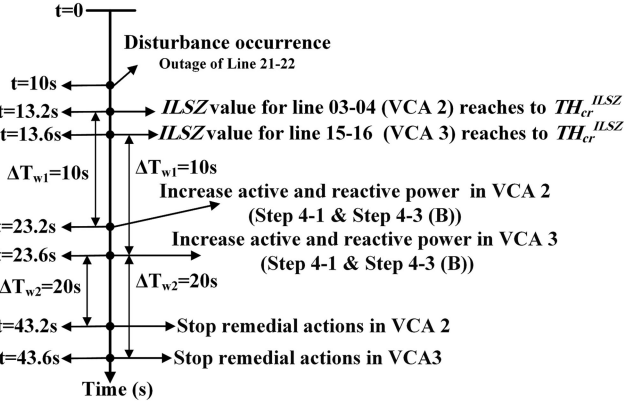Fig. 7.   Evolution of bus voltages in scenario 1 with proposed SPS.

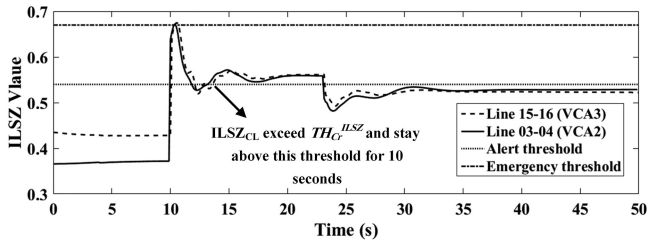Fig. 8.   Control actions executed by the proposed scheme in scenario 1.

Fig. 9.   ILSZ values for critical line 15–16 in VCA 3 and line 3–4 in VCA2 (scenario 1).
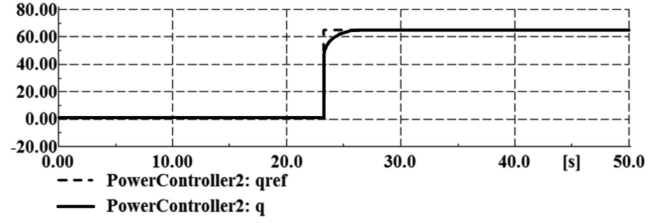

Fig. 10.   Proposed SPS changes the reactive power generation of PV resource located at bus 12 (scenario 1).
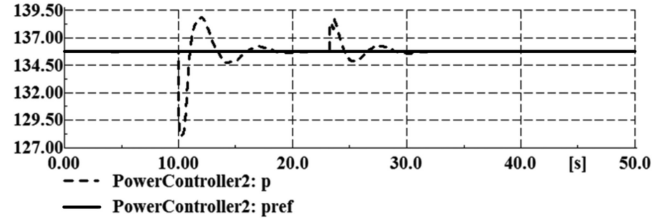

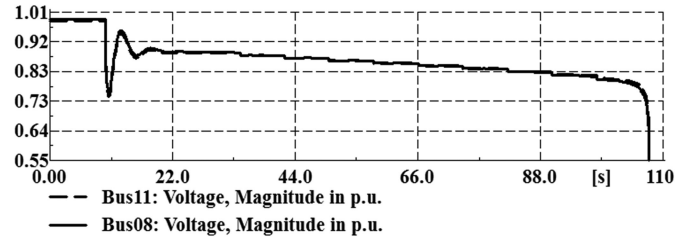Fig. 11.   Evolution of bus voltages in scenario 2 without proposed SPS.

Fig. 12.   Evolution of bus voltages in scenario 2 with proposed SPS.
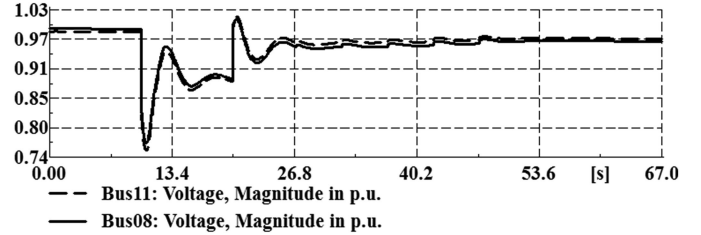
Figs. 8 and 9, after the event, the values of ILSZ for line 3–4 in VCA 2 and line 15–16 in VCA 3 exceeded TH_{cr}^{ILSZ}, which caused the generation rescheduling procedure (i.e., step 4 of the proposed scheme) to increase the active power of G3 by 25 MW to compensate an active power shortage in VCA. Also, since V_{CBs} became $< \mathrm{TH}_{cr}^{LV}$ (see Fig. 7), the reactive power of G3 and PV (see Fig. 10) resources located in VCA 2 increased simultaneously to prevent the voltage drop. Similarly, to maintain voltage stability in VCA 3, the active power of G4 and G6, and the reactive power of VLSPVPP in this area increased to provide the required active/reactive power. Finally, performing these remedial actions caused the ILSZ values of critical lines to become $< \mathrm{TH}_{cr}^{ILSZ}$ again, and all bus voltages became $> \mathrm{TH}_{alrt}^{LV}$. Therefore, without any load shedding, the proposed SPS caused the system to reach a stable OP in < 25 s after starting the remedial actions.

B. Analyzing Performance of the Proposed SPS Against Outage of G3 in IEEE 39-Bus Test System (Scenario 2)

This scenario analyzed the effect of a generator G3 outage on the voltage stability status of the modified IEEE 39-bus test system. This disturbance occurred at $t = 10$ s and resulted in voltage instability, which is shown in Fig. 11. According to this figure, at $t = 40$ s, $t = 60$ s, and $t = 94$ s, AVRs of G9, G5, and G7, respectively, reached their limits. Also, voltage drop caused some OLTCs to automatically change their tap positions to improve voltage profile. However, these changes resulted in more voltage drop and led to activation of over-excitation limiters of generators G6 and G1. Eventually, voltage collapse occurred at $t = 108$ s.

Fig. 12 shows that applying the proposed algorithm can properly prevent the OP to leave the region of attraction and cause the network to reach a stable equilibrium point. As shown in Figs. 13 and 14, after the event occurrence, ILSZ values for line 3–4 (in VCA 2) and line 15–16 (in VCA 3) exceeded TH_{cr}^{ILSZ}, which
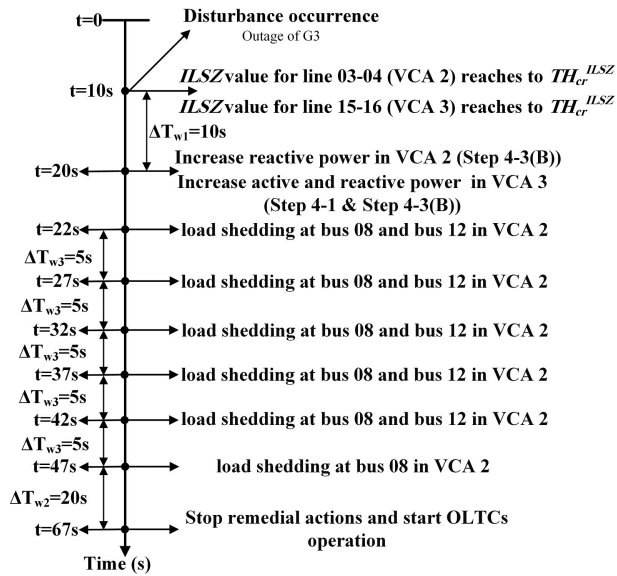
This article has been accepted for inclusion in a future issue of this journal. Content is final as presented, with the exception of pagination.

KHOSHKHOO *et al.*: REMEDIAL ACTION SCHEME TO PREVENT MID/LONG-TERM VOLTAGE INSTABILITIES

9

Fig. 13.   Control actions executed by the proposed scheme in scenario 2.

Fig. 15.   Modified version of Nordic32 test system used in scenario 3.

Fig. 14.   ILSZ values for critical line 15–16 in VCA 3 and line 3–4 in VCA2 (scenario 2).

Fig. 16.   Evolution of bus voltages without proposed SPS in scenario 3.
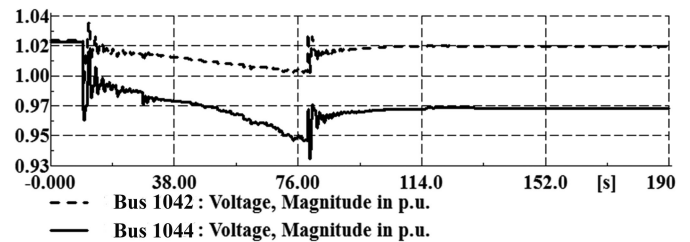
Fig. 17.   Evolution of bus voltages with proposed SPS in scenario 3.

initiated the SPS. In this respect, since V_{CBs} became $< \text{TH}_{cr}^{\text{LV}}$ (see Fig. 12), the reactive power of PV resources located in VCA 2 increased simultaneously to prevent the voltage drop. It should be stated that in VCA 2, SGs reached their limits and could not generate any more active power.

To compensate the power shortage in VCA 3, the total active power generation of G4 and G6 increased by 60^{MW}. Also, since V_{CBs} (in VCA 3) became $< \text{TH}_{cr}^{\text{LV}}$, the reactive power generation of all VLSPVPP in this area increased (at $t = 20$ s) to rapidly improve the voltage stability. However, performing these remedial actions could not cause ILSZ values and bus voltages to reach acceptable limits. Therefore, step 5 of the proposed SPS started at $t = 22$ s, which totally shed 65^{MW} (0.95% of total system loading) of loads at bus 12 (the nearest load to the critical bus 11) and bus 08 to increase V_{CBs} above $\text{TH}_{\text{alrt}}^{\text{LV}}$ and decrease ILSZ values of critical lines below TH_{cr}^{ILSZ}. Eventually, the system reached a stable OP before $t = 50$ s.

C. Analyzing the Performance of the Proposed SPS Against the Outage of Line 4032–4044 in Nordic32 Test System (Scenario 3)

In this section, a modified version of the Nordic32 test system [40] is used to analyze the performance of the proposed SPS.
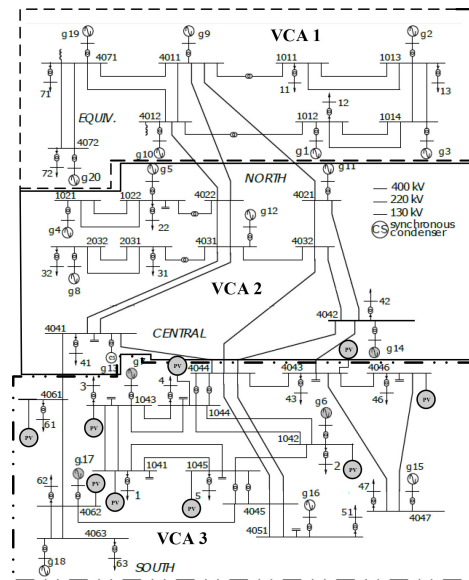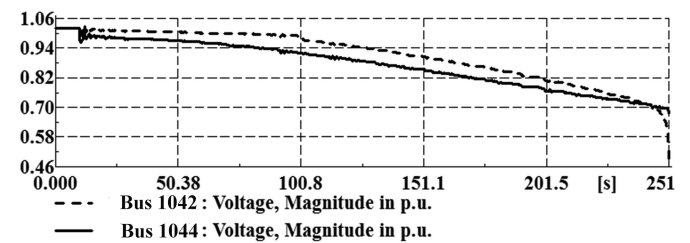
This network was divided into three VCAs and all utility-scale PV resources were installed in VCA3 (with a penetration level of 25%), shown in Fig. 15. Evolution of the bus voltages after the outage of line 4032–4044 at $t = 10$ s is given in Fig. 16, which shows that the event led to voltage collapse at about $t = 251$ s. However, Fig. 17 shows that applying the proposed algorithm can properly prevent the OP to leave the region of attraction and maintain system stability. According to Fig. 18, after the disturbance occurrence that caused the ILSZ value for line 4045–4062 (in VCA3) to exceed TH_{cr}^{ILSZ}, unlike ROCOF, ROCOV became $> \text{TH}_{cr}^{\text{ROCOV}}$ for ΔT_{ROCOV}s. Therefore, the proposed scheme increased the reactive power generation of VLSPVPP and some SGs (i.e., G16, G17, and G18, whose RPRI was $> \text{TH}_{cr}^{\text{RPRI}}$) to provide the required reactive power. Finally, ILSZ values of the critical lines became $< \text{TH}_{cr}^{ILSZ}$ and bus
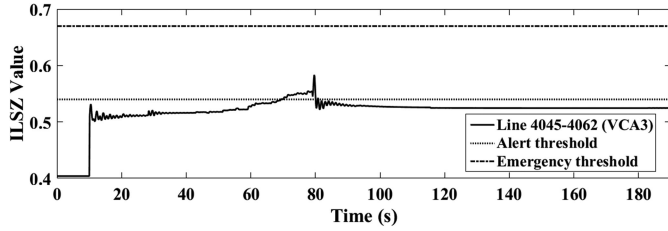
Fig. 18.   ILSZ value for the critical line 4045–4062 in scenario 3.
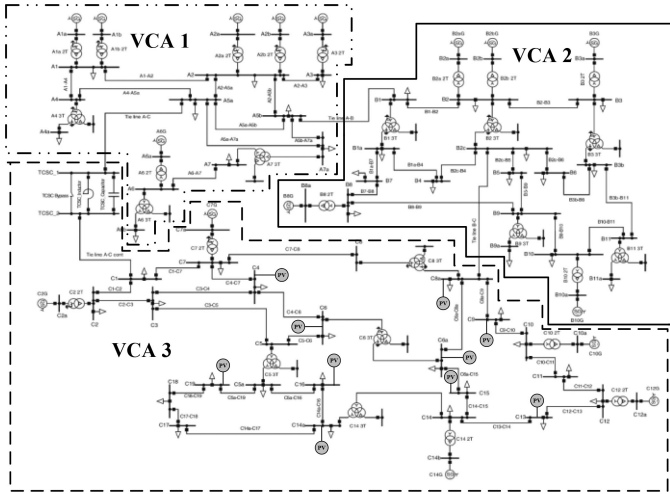
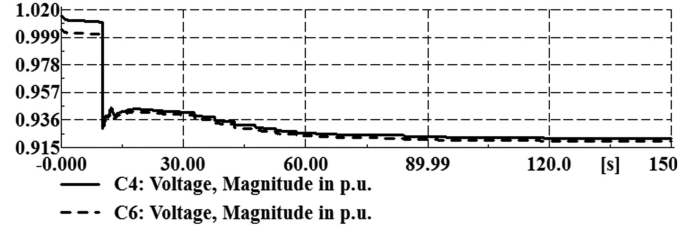Fig. 19.   In the PST 16 test system, all PV resources were installed in VCA 3.

Fig. 20.   Evaluation of bus voltages in scenario 4 without proposed SPS.
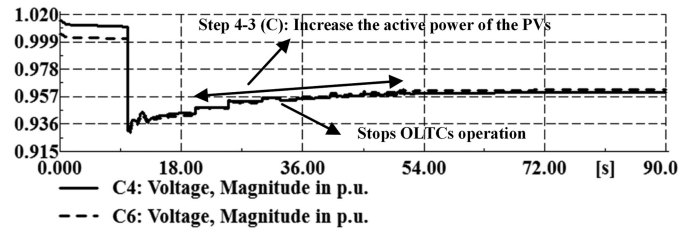

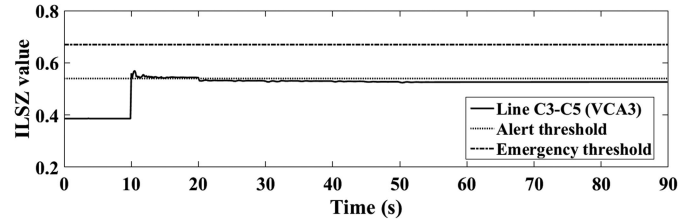Fig. 21.   Evolution of bus voltages with the proposed SPS in scenario 4.

Fig. 22.   ILSZ value for critical line C3–C5 in VCA 3 (scenario 4).

voltages exceeded $\text{TH}_{\text{alrt}}^{\text{LV}}$, which meant that the system reached a stable OP in < 34 s after starting the corrective remedial actions (without any load-shedding).

D. Analyzing the Performance of the Proposed SPS Against the Load Disturbance in PST 16 (Scenario 4)

In this section, the performance of the proposed SPS is investigated against load disturbance in the PST 16 test system [41]. To properly simulate the dynamic behavior of the network, all SGs were represented with a sixth-order model and equipped with AVRs and governors. Also, OLTCs were used to connect voltage-dependent loads to the power system.

As mentioned in Section II, in this network, which includes three VCAs, the criterion "SVSI>0.8" was used to determine weak buses in each area to install VLSPVPP.

In this respect, since all weak buses were located in VCA3, these renewable resources were installed in the weak buses of VCA 3 (with a penetration level of 25%), shown in Fig. 19.

In this scenario, the performance of the proposed scheme against load disturbances is analyzed.

As shown in Fig. 19, following a 10% increase in the apparent power of all loads in VCA 3 at $t = 10$ s, the bus voltages in VCA 3 rapidly decreased. Also, the operation of some OLTCs (C6, C4, C3, C6a, and C15), which tried to improve the voltage at load buses, adversely affected stability status and decreased the bus voltages. Finally, as shown in Fig. 20, bus voltages remained below the threshold $\text{TH}_{cr}^{\text{LV}}$.

Considering the proposed SPS, the disturbance occurrence caused the ILSZ value of line C3–C5 to exceed TH_{cr}^{ILSZ}, and initiate the proposed SPS. Since, following the disturbance occurrence, V_{CBs} were $> \text{TH}_{cr}^{\text{LV}}$, step 4–3 of the proposed algorithm determined the most critical bus (i.e., bus C6), and, starting from the nearest resource to this bus, increased the reactive power output of PV resources one by one (i.e., PVs at buses C6, C4, C6a, C19, C16, C8a, and, finally, C15), which caused the ILSZ values of any lines to become $< \text{TH}_{cr}^{ILSZ}$ and all bus voltages to become $> \text{TH}_{\text{alrt}}^{\text{LV}}$. Eventually, as shown in Figs. 21 and 22, without any load shedding, the proposed SPS caused the system to reach a stable OP in < 25 s. It should be noted that, in this procedure, to avoid over-voltage, the reactive power of PVs at C16, C8a, and C15 were increased by only 50%. Also, since RPRI values of all SGs in VCA 3 were $< \text{TH}_{cr}^{\text{RPRI}}$, they could not generate any more reactive power.

E. Comparison With the Conventional Control System

In this section, the performance of the proposed SPS against the outage of line 4032–4044 in the Nordic32 test system, analyzed in Section IV-C is compared with those presented in [6] and [42]. Table V gives the results of this comparison, which indicates that the proposed method was able to maintain system stability without any load shedding, and the OP reached a stable equilibrium point more quickly.

This article has been accepted for inclusion in a future issue of this journal. Content is final as presented, with the exception of pagination.

KHOSHKHOO *et al.*: REMEDIAL ACTION SCHEME TO PREVENT MID/LONG-TERM VOLTAGE INSTABILITIES 11

TABLE V
COMPARISON OF THE PROPOSED SPS AND THOSE PRESENTED IN [6] AND [42]

	The method proposed in		
	This paper	[6]	[42]
Load shedding amount	0	310 ^{MW}	380 ^{MW}
The time required to reach an equilibrium point	94 s	195 s	215 s

V. CONCLUSION

In this article, an efficient SPS to preventive mid-term and long-term voltage instability has been proposed. The proposed method uses generation rescheduling and load shedding procedures in which, considering the local nature of volt/var control, the ED concept is used to select the optimal remedial actions with the highest impacts on the stability status. Since the proposed method does not use optimization algorithms, which usually have a high computational burden, it is able to quickly select and perform efficient remedial actions to bring the OP back into the Normal state as soon as possible. Also, to assess the ability of utility-scale PV resources to improve system stability, in generation rescheduling procedures, the proposed algorithm uses VLSPVPP, which is able to quickly change its generation and effectively improve voltage stability status. Dynamic simulations results performed in IEEE 39-bus, Nordic32, and PST 16 test systems, and their comparison with some previously published methods, show the effectiveness of this method in timely executing appropriate and coordinated remedial actions and significantly decreasing the required load shedding amount to maintain the system stability.

REFERENCES

[1] H. Khoshkhoo and S. Shahrtash, "On-line dynamic voltage instability prediction based on decision tree supported by a wide-area measurement system," *IET Gener. Trans. Distrib.*, vol. 6, no. 11, pp. 1143–1152, Nov. 2012.
[2] Y. Siavash, H. Khoshkhoo, and S. M. Shahrtash, "Generation Equivalence Index (GEI) to assign low-order models to synchronous generators in voltage security assessment based on dynamic simulation," *Int. J. Elect. Power Energy Syst.*, vol. 123, 2020, doi: 10.1016/j.ijepes.2020.106274.
[3] P. Aghdam, and H. Khoshkhoo, "Voltage stability assessment algorithm to predict power system loadability margin," *IET Gen. Trans. Distrib.*, vol. 14, no. 10, 1816–1828, May. 2020.
[4] M. J. Hossain, H. R. Pota, M. A. Mahmud, and R. A. Ramos, "Investigation of the impacts of large-scale wind power penetration on the angle and voltage stability of power systems," *IEEE Syst. J.*, vol. 6, no. 1, pp. 76–84, Mar. 2012.
[5] M. A. Azzouz, H. E. Farag, and E. F. El-Saadany, "Real-time fuzzy voltage regulation for distribution networks incorporating high penetration of renewable sources," *IEEE Syst. J.*, vol. 11, no. 3, pp. 1702–1711, Sep. 2014.
[6] S. R. Islam, D. Sutanto, and K. M. Muttaqi, "Coordinated decentralized emergency voltage and reactive power control to prevent long-term voltage instability in a power system," *IEEE Trans. Power Syst.*, vol. 30, no. 5, pp. 2591–2603, Dec. 2015.
[7] Special protection systems (SPS) and remedial action schemes (RAS): Assessment of definition, regional practices, and application of related standards," North Amer. Elect. Rel. Corp., Atlanta, GA, USA, Apr. 2013.
[8] M. Arabzadeh, H. Seifi, and M. K. Sheikh-El-Eslami, "A new mechanism for remedial action schemes design in a multi-area power system considering competitive participation of multiple electricity market players," *Int. J. Elect. Power Energy Syst.*, vol. 103, pp. 31–42, Dec. 2018.
[9] A. Parizad, A. H. Khoshkhoo, S. Dehghan, and R. Moradtalab, "An intelligent load and generation shedding procedure in an islanded network using a smart power management system," in *Proc. IEEE Smart Grid Conf.*, Dec. 2017, pp. 1–12.
[10] A. Parizad and H. Khoshkhoo, "Dynamic stability improvement of islanded power plant by smart power management system—principles, descriptions and scenarios," in *Advanced Smart Grid Functionalities Based on PowerFactory*. Berlin, Germany: Springer, 2018, ch. 8, pp. 181–209.
[11] Z. Li, G. Geng, and Q. Jiang, "Transient stability emergency control using asynchronous parallel mixed-integer pattern search," *IEEE Trans. Smart Grid*," vol. 9, no. 4, pp. 2976–2985, Jul. 2018.
[12] E. Ghahremani, A. Heniche, M. Perron, M. Racine, S. Landry, and H. Akremi, "A detailed presentation of an innovative local and wide-area special protection scheme to avoid voltage collapse: From proof of concept to grid implementation," *IEEE Trans. Smart Grid*, vol. 10, no. 5, pp. 5196–5211, Sep. 2019.
[13] D.-H. Choi, S. H. Lee, Y. C. Kang, and J.-W. Park, "Analysis on special protection scheme of Korea electric power system by fully utilizing statcom in a generation side," *IEEE Trans. Power Syst.*, vol. 32, no. 3, pp. 1882–1890, Aug. 2017.
[14] M. D. Maram and N. Amjady, "Event-based remedial action scheme against super-component contingencies to avert frequency and voltage instabilities," *IET Gener. Trans. Distrib.*, vol. 8, no. 9, pp. 1591–1603, Apr. 2014.
[15] M. Derafshian, N. Amjady, and S. Dehghan, "Special protection scheme against voltage collapse," *IET Gener. Trans. Distrib.*, vol. 10, no. 2, pp. 341–351, Feb. 2016.
[16] Y. Xu, Z. Y. Dong, F. Luo, R. Zhang, and K. P. Wong. "Parallel-differential evolution approach for optimal event-driven load shedding against voltage collapse in power systems," *IET Gener. Trans. Distrib.*, vol. 8, no. 4, pp. 651–660, Dec. 2013.
[17] D. P. Manjure and E. B. Makram, "Optimal load curtailment as a bi-criteria program," *Elect. Power Syst. Res.*, vol. 66, no. 2, pp. 155–161, Aug. 2003.
[18] T. Amraee, A.M. Ranjbar, R. Feuillet, and B. Mozafari. "System protection scheme for mitigation of cascaded voltage collapses," *IET Gener. Trans. Distrib.*, vol. 3, no. 3, pp. 242–256, Mar. 2009.
[19] Y. Wang, I. R. Pordanjani, W. Li, W. X. Xu, and E. Vaahedi. "Strategy to minimise the load shedding amount for voltage collapse prevention," *IET Gener. Trans. Distrib.*, vol. 5, no. 3, pp. 307–313, Mar. 2011.
[20] Y. T. Chou, Y. J. Wang, C. H. Hsieh, R. Y. Wang, and S. K. Shah. "Study of stability indices for special protection system in Taiwan," in *Proc. 10th Int. Conf. Intell. Inf. Hiding Multimedia Signal Process.*, 2014, pp. 815–818.
[21] M. Abedini, M. Sanaye-Pasand, and S. Azizi. "Adaptive load shedding scheme to preserve the power system stability following large disturbances," *IET Gener. Trans. Distrib.*, vol. 8, no. 12, pp. 2124–2133, Jul. 2014.
[22] S. Yari and H. Khoshkhoo, "An effective corrective remedial action algorithm to prevent voltage instability," in *Proc. 5th Conf. Knowl. Based Eng. Innov.*, 2019, pp. 460–466.
[23] M. M. Aman, M. Arshad, H. K. Zuberi, and J. A. Laghari. "A hybrid scheme of load shedding using globalized frequency and localized voltage (GFLV) controller," *Int J. Electr. Power Energy Syst.*, vol. 113, pp. 674–685, Dec. 2019.
[24] Renewables, Int. Energy Agency, Paris, France, 2018 [Online]. Available: https://www.iea.org/renewables2018/power/
[25] Solar energy, Int. Energy Agency, 2019. [Online]. Available: https://www.iea.org/topics/renewables/solar/
[26] A. Cabrera-Tobar, E. Bullich-Massague, M. Aragüés-Peñalba, and O. Gomis-Bellmunt, "Review of advanced grid requirements for the integration of large scale photovoltaic power plants in the transmission system," *Renew. Sustain. Energy Rev.*, vol. 62, pp. 971–987, Sep. 2016.
[27] R. Shah, N. Mithulananthan, R. Bansal, and V. Ramachandaramurthy, "A review of key power system stability challenges for large-scale PV integration," *Renew. Sustain. Energy Rev.*, vol. 41, pp. 1423–1436, Jan. 2015.
[28] M. Kabir, Y. Mishra, G. Ledwich, Z. Xu, and R. Bansal, "Improving voltage profile of residential distribution systems using rooftop PVs and battery energy storage systems," *Appl. Energy*, vol. 134, pp. 290–300, Dec. 2014.
[29] M. A. Eltawil and Z. Zhao, "Grid-connected photovoltaic power systems: Technical and potential problems—A review," *Renew. Sustain. Energy Rev.*, vol. 14, no. 1, pp. 112–129, Jan. 2010.
[30] S. Eftekharnejad, V. Vittal, G. T. Heydt, B. Keel, and J. Loehr, "Impact of increased penetration of photovoltaic generation on power systems," *IEEE Trans. Power Syst.*, vol. 28, no. 2, pp. 893–901, Oct. 2013.
[31] F. Karbalaei and H. Shahbazi, "Determining an appropriate partitioning method to reduce the power system dimensions for real time voltage control," *Int. J. Elect. Power Energy Syst.*, vol. 100, pp. 58–68, Sep. 2018.

This article has been accepted for inclusion in a future issue of this journal. Content is final as presented, with the exception of pagination.

12   IEEE SYSTEMS JOURNAL

[32] M. Shahidehpour and Y. Wang, *Communication and Control in Electric Power Systems: Applications of Parallel and Distributed Processing*. Hoboken, NJ, USA: Wiley, 2004.

[33] J. Zhong, E. Nobile, A. Bose, and K. Bhattacharya, "Localized reactive power markets using the concept of voltage control areas," *IEEE Trans. Power Syst.*, vol. 19, no. 3, pp. 1555–1561, Aug. 2004.

[34] S. Pérez-Londoño, L. Rodríguez, and G. Olivar, "A simplified voltage stability index (SVSI)," *Int. J. Elect. Power Energy Syst.*, vol. 63, pp. 806–813, 2014.

[35] S. Yari and H. Khoshkhoo, "A comprehensive assessment to propose an improved line stability index," *Int. Trans. Elect. Energy Syst.*, vol. 29, no. 4, Jan. 2019, Art. no. e2806.

[36] S. Yari and H. Khoshkhoo, "Assessment of line stability indices in detection of voltage stability status," in *Proc. IEEE Int. Conf. Environ. Elect. Eng. IEEE Ind. Commercial Power Syst. Eur.*, 2017, pp. 1–5.

[37] L. Wang, Y. Liu, and Z. Luan, "Power transmission paths based voltage stability assessment," in *Proc. Transmiss. Distrib. Conf. Exhib., Asia Pac.*, 2005, pp. 1–5.

[38] B.-I. Crăciun, T. Kerekes, D. Séra, and R. Teodorescu, "Overview of recent grid codes for PV power integration," in *Proc. 13th Int. Conf. Optim. Elect. Electron. Equip.*, 2012, pp. 959–965.

[39] A. Yazdani and R. Iravani, *Voltage-Sourced Converters in Power Systems: Modeling, Control, and Applications*. Piscataway, NJ, USA: IEEE Press, 2012.

[40] G. Lammert, D. Premm, L. D. P. Ospina, J. C. Boemer, M. Braun, and T. Van Cutsem, "Control of photovoltaic systems for enhanced short-term voltage stability and recovery," *IEEE Trans. Energy Convers.*, vol. 34, no. 1, pp. 243–254, Oct. 2019.

[41] F. M. Gonzalez-Longatt and J. L. Rueda, *PowerFactory Applications For Power System Analysis*. Berlin, Germany: Springer, 2014.

[42] D. A. Panasetsky and N. I. Voropai, "A multi-agent approach to coordination of different emergency control devices against voltage collapse," in *Proc. IEEE Bucharest PowerTech.*, 2009, pp. 1–7.

Hamid Khoshkhoo received the B.S. degree from Zanjan University, Zanjan, Iran, in 2005, the M.S. degree from Amirkabir University of Technology, Tehran, Iran, in 2007, and the Ph. D. degree from Iran University of Science and Technology, Tehran, Iran in 2014, all in electrical power systems.

He is currently an Assistant Professor with Sahand University of Technology, Tabriz, Iran, where he is supervising Ph.D. and master's candidates. He has been a Principal Investigator in several research and industrial projects and his focus is including power system stability, power system protection, and renewable energy integration.

Siavash Yari received the M.S. degree in electrical engineering from Sahand University of Technology, Sahand, Iran, in 2018.

He is currently a Research Assistant with Sahand University of Technology. His research interests include power system voltage stability and renewable energy integration.

Aref Pouryekta (Member, IEEE) received the Ph.D. degree in electrical engineering from Tenaga National University, Kajang, Malaysia, in 2017.

He has been a Postdoctoral Research with Tenaga National University. He is currently a Senior Consultant in DNV GL, Clean Technology Centre, Singapore. His research interests include renewable energy integration, microgrid stability, and power system modeling.

Vigna K. Ramachandaramurthy (Senior Member, IEEE) received the bachelor's degree in electrical and electronics engineering under the Malaysian Government Scholarship, and the Ph. D. degree in electrical engineering from the University of Manchester Institute of Science and Technology (UMIST), Manchester, U.K., in 1998 and 2001, respectively.

In 2002, he was an Electrical Engineer with the Malaysian Electrical Utility, Tenaga Nasional Berhad. In 2005, he moved to Universiti Tenaga Nasional, where he is currently a Professor with the Institute of Power Engineering. He is currently a Chartered Engineer registered with the Engineering Council of U.K., and a Professional Engineer registered with the Board of Engineers, Malaysia. He is also the Principal Consultant for Malaysia's biggest electrical utility, Tenaga Nasional Berhad. He has completed more than 250 projects in renewable energy. He has also developed several technical guidelines for interconnection of distributed generation and solar PV in Malaysia. He is very active in industrial consultancy projects and has supervised and graduated more than 100 postgraduate candidates. His research interests include power systems related studies, renewable energy, energy storage; power quality, electric vehicle, and rural electrification.

Dr. Ramachandaramurthy is the Editorial Board/Associate Editor for the *IET Smart Grid, IET Renewable Power Generation*, the IEEE SMART GRID, and IEEE ACCESS. He is the recipient of many awards for research and leadership, such as the Institution of Engineering and Technology Mike Sargeant Award, the Institution of Engineers Malaysia Young Engineers Award.

Josep M. Guerrero (Fellow, IEEE) received the B.S. degree in telecommunications engineering, the M.S. degree in electronics engineering, and the Ph.D. degree in power electronics from the Technical University of Catalonia, Barcelona, Spain, in 1997, 2000, and 2003, respectively.

Since 2011, he has been a Full Professor with the Department of Energy Technology, Aalborg University, Aalborg, Denmark, where he is responsible for the Microgrid Research Program. Since 2014, he has been a Chair Professor with Shandong University, Jinan, China. Since 2015, he has been a Distinguished Guest Professor with Hunan University, Changsha, China. Since 2016, he is a Visiting Professor Fellow with Aston University, Birmingham, U.K., and a Guest Professor with the Nanjing University of Posts and Telecommunications, Nanjing, China. Since 2019, he has been a Villum Investigator with The Villum Fonden, which supports the Center for Research on Microgrids, Aalborg University. His research interests include different microgrid aspects, including power electronics, distributed energy-storage systems, hierarchical and cooperative control, energy management systems, smart metering, and the Internet of Things for ac/dc microgrid clusters and islanded minigrids, and specially focused on microgrid technologies applied to offshore wind, maritime microgrids for electrical ships, vessels, ferries, and seaports, and space microgrids applied to nanosatellites and spacecrafts.

Dr. Guerrero is an Associate Editor for a number of IEEE Transactions. He was the recipient of the Best Paper Award of the *Journal of Power Electronics* in 2016. For six consecutive years, from 2014 to 2019, he was also the recipient of Highly Cited Researcher by Clarivate Analytics (former Thomson Reuters).